Intraplate stress state from finite element modelling: The southern border of the Spanish Central System

S. Martín-Velázquez [a,*], G. de Vicente [b], F.J. Elorza [c]

[a] Department of Biology and Geology, Rey Juan Carlos University, Tulipán s/n, Móstoles, 28933 Madrid, Spain
[b] Department of Geodynamics, Complutense University of Madrid, José Antonio Novais s/n, 28040 Madrid, Spain
[c] Department of Applied Mathematics and Computer Methods, Technical University of Madrid, Ríos Rosas 21, 28003 Madrid, Spain

article info

Article history:
Received 6 August 2008
Received in revised form 9 March 2009
Accepted 23 March 2009
Available online xxxx

Keywords:
Reference states of stress
Tectonic stresses
Stress modelling
Gravity modelling
Iberian Peninsula

abstract

An elastic finite element approach has been used with the dual aim of determining the most appropriate reference state of stress, namely a uniaxial strain state or a lithostatic state, and refining the understanding of the Iberian intraplate stresses. A cross-section model with an average crustal rheology and a flat topography has been analysed first in order to evaluate the influence of boundary conditions and rheological properties in the reference and tectonic stress states. The uniaxial and lithostatic states are obtained by including the overburden weight and a compressive horizontal load, which equals the uniaxial and lithostatic stress respectively, and provided that Poisson's ratio equals ~0.5 in the lithostatic state. On the other hand, a tectonic state with a $\sigma_H N \sigma_V$ regime is reproduced by adding a horizontal constant load. Subsequently, constraints on the magnitude of the predicted Cenozoic stresses along a NW–SE cross-section in the southern border of the Spanish Central System (in the Variscan granitic basement of El Berrocal) have been estimated incorporating the topographic loading, lithological variations and the most recent far tectonic stresses. The deep geological structure has been established from gravity modelling and geological data. To simulate the active strike-slip to uniaxial extension regimes in the interior of Iberian Peninsula, a lithostatic initial state has to be considered and a tectonic load in the range of 15–20 MPa has to be applied. The gradient of maximum horizontal stress originated under these conditions is in the range of 3–9 MPa km^{-1}. These results are in accordance with the estimated intraplate tectonic stress, the force along the convergent plate boundary of Eurasia–Africa, the lithospheric strength of Iberia, and the direct measurements of stresses.

1. Introduction

An important problem when estimating the stress magnitudes lies in the lack of a single reference state of stress, as the quantification of stresses, which are intimately related to tectonics, can be very different. Among others, the uniaxial strain state or the lithostatic state (according to the terms in Engelder, 1993) has been used to solve the stresses in a lithosphere assumed to be elastic (McGarr and Gay, 1978; Turcotte and Schubert, 1982; McGarr, 1988; Twiss and Moores, 1992; Engelder, 1993; Ranalli, 1995). Although the use of these reference states is sometimes justified in the scientific literature, they are usually assumed or described, without indicating which of them is the most suitable. As a result, this issue remains still a subject of controversy in the scientific community (e.g. Carminati et al., 2004). On the other hand, in situ measurements in deep boreholes indicate higher horizontal than vertical stresses (McGarr and Gay, 1978; Brudy et al., 1997; Reynolds et al., 2006), and both reference states represent, at best, incomplete approaches to lithospheric stresses. Several natural processes can modify the reference state, such as tectonic stresses arising from plate boundaries, topographic loading, unloading due to erosion, lithospheric bending, thermoelastic loads, and pore fluid pressure (Turcotte and Schubert, 1982; Twiss and Moores, 1992; Engelder, 1993; Caputo, 2005). Various authors have addressed the notion of the reference tectonic state in order to evaluate the relative importance of local and far field sources of stress in the intraplate lithosphere from variations of the gravitational potential energy (Zhou and Sandiford, 1992; Coblentz et al., 1994; Coblentz and Sandiford, 1994).

Intraplate stress information is essential for understanding the sources of stress responsible for lithospheric deformation. Work on recent stresses in the Iberian Peninsula are centred both on the orientation of the stress tensor, from stress inversion methods of fault-slip data and/or earthquake focal mechanism solutions (Galindo-Zaldívar et al., 1993; De Vicente et al., 1996; Ribeiro et al., 1996; Herraiz et al., 2000; Stich et al., 2006; De Vicente et al., 2008), and on its magnitude, either by means of stress relief measurements (González de Vallejo et al., 1988; Jurado and Müller, 1997; Schindler et al., 1998) or by numerical methods of stress–strain calculation (Gölke and Coblentz, 1996; Carminati et al., 1998; Andeweg et al., 1999; Cloetingh

* Corresponding author. Fax: +34 91 664 74 90.
E-mail address: silvia.martin@urjc.es (S. Martín-Velázquez).

doi: 10.1016/j.tecto.2009.03.024

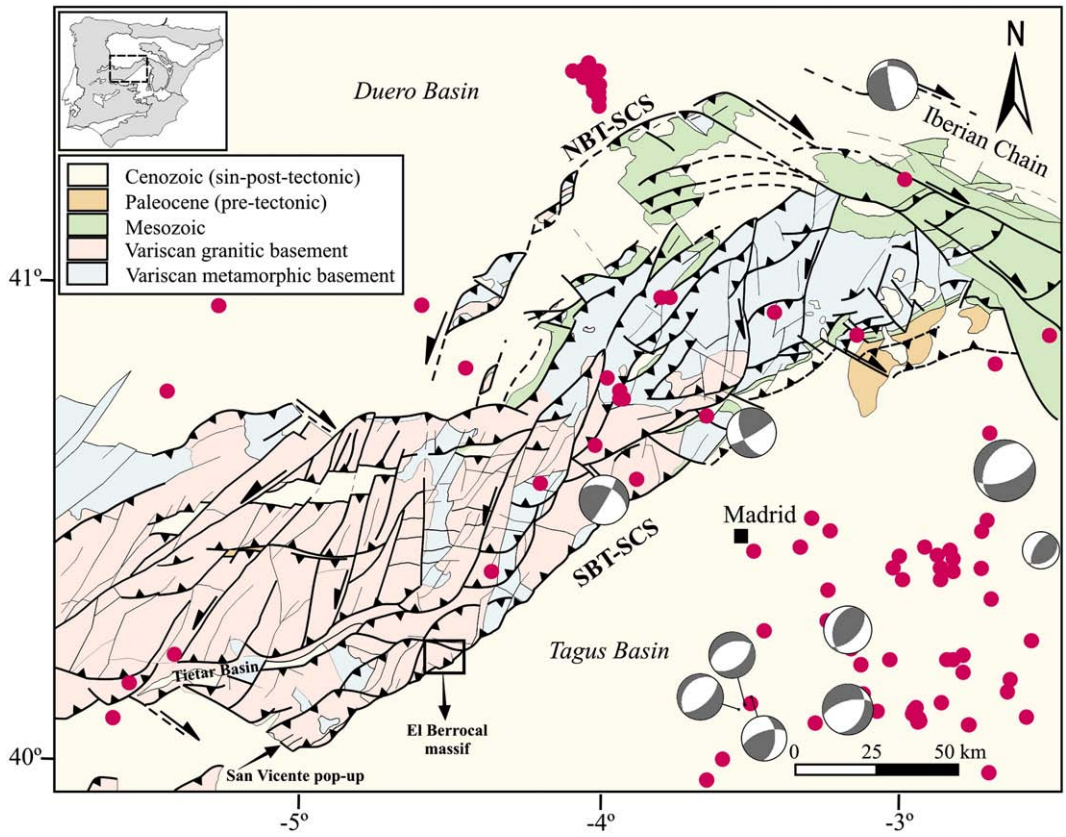

Fig. 1. Geological sketch of the Spanish Central System, with the distribution of earthquakes (dots) and focal mechanisms (for details see De Vicente et al., 2007). The El Berrocal massif (box) is located within the NE–SW sector, on the part which is closest to the E–W sector. NBT-SCS is the Northern Border Thrusts of the Spanish Central System, and SBT-SCS is the Southern Border Thrust of the Spanish Central System. Top left corner: mountainous range (grey tones) and alpine basins (white) with location of the Spanish Central System within Iberia.

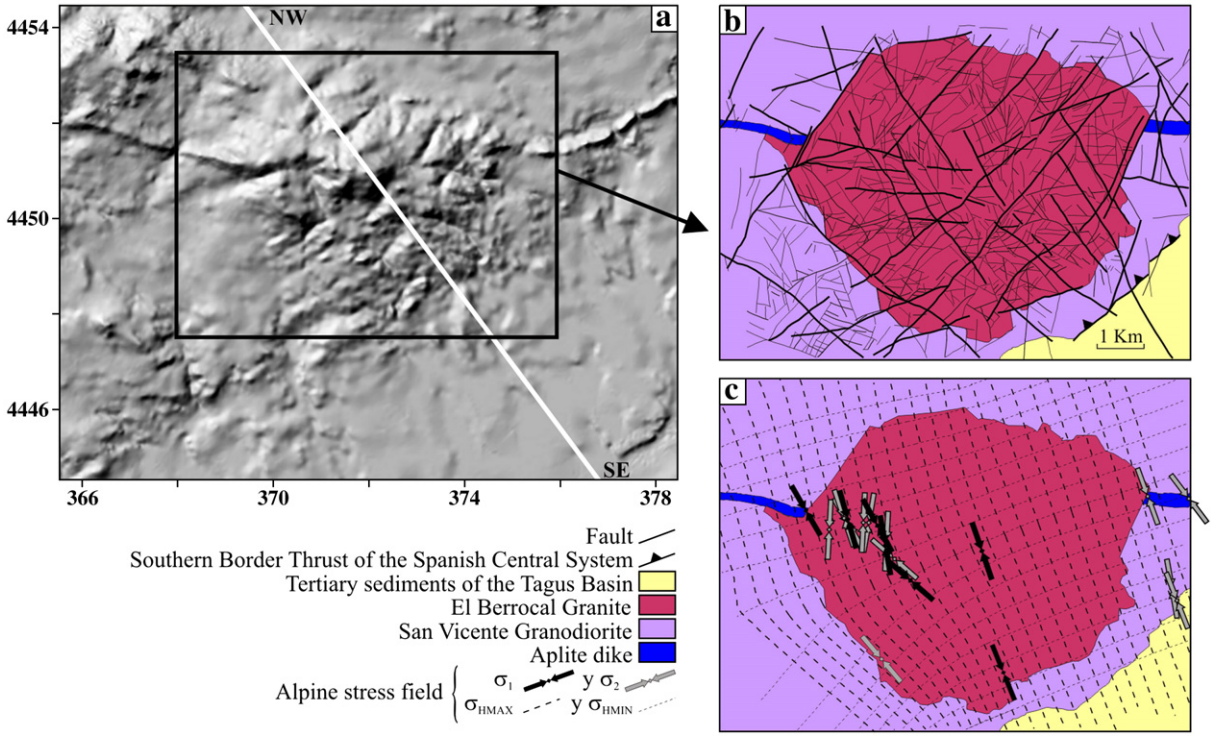

Fig. 2. a) Digital elevation model (pixel 50 × 50 m) of the El Berrocal massif used to obtain the topography of the modelled crustal section (based on the topographical maps, scale 1:50.000, Geographical Service of the Spanish Army sheets 579, 580, 602, and 603). UTM coordinates (kilometres) referred to zone 30. The NW–SE line indicates the profile orientation of the gravity and stress modelling. b) Geological map of the El Berrocal massif with the main lithological bodies and fracture network. c) Map of Alpine stress field depicting maximum horizontal stress (σ_{HMAX}) and minimum horizontal stress (σ_{HMIN}) trajectories obtained from fault population analysis. σ_1 is the horizontal projection of the maximum principal stress in strike-slip tensors. σ_2 is the horizontal projection of the intermediate principal stress in tensional tensors. Modified from CSN (2000).

Please cite this article as: Martín-Velázquez, S., et al., Intraplate stress state from finite element modelling: The southern border of the Spanish Central System, Tectonophysics (2009), doi:10.1016/j.tecto.2009.03.024

et al., 2002; Jiménez Munt and Negredo, 2003). The knowledge of the stress regime in the Spanish Central System is exhaustive (De Vicente et al., 1996; Herraiz et al., 2000; De Vicente et al., 2007) but detailed studies on the stress magnitudes (direct measurements, numerical methods) are not available. For this reason, a stress analysis by means of the finite element technique along a NW–SE vertical profile that crosses the Southern Thrust of the Spanish Central System at the granitic massif of El Berrocal, on the south-western border of this structure, is presented here. We have chosen this area because of the numerous and available geological information. The El Berrocal massif contains an important uranium mineralization system and several studies have been carried out in order to describe its structural, lithological, geochemical, hydrogeochemical and hydrogeological aspects, with the aim of understanding the natural processes of radionuclide migration in a fractured granitic environment (Campos et al., 1996; Pérez del Villar et al., 1996; CSN, 2000; Pérez-López et al., 2005; Gómez et al., 2006). The petrological, geophysical, structural and recent stress information of this intraplate mountainous region (De Vicente et al., 1996; CSN, 2000; Pérez-López et al., 2005) has been used to build a model geometry with well differentiated lithological bodies and to allow an adequate restriction on boundary conditions. A zone with a clear heterogeneity in the Variscan basement has been selected in order to assess the influence of such in the stress distribution. The results of the modelling will complete the stress data in this area with their distribution with depth and with the magnitude of the intraplate tectonic stress.

The finite element code that has been used, Ansys (Swanson Analysis Systems, Inc.), allows the efficient calculation of the magnitude and orientation of stresses, displacements and/or deformations in a given continuous body with some specific mechanical properties and boundary conditions (Zienkiewicz and Taylor, 1994). Comparison of the results obtained by means of numerical models with the stress data and/or deformations observed in the lithosphere constitutes a very useful way of understanding the geodynamical processes at different scales. The quantification of the stress magnitudes and their depth distribution have to be consistent with deformation processes in the lithosphere (Gölke et al., 1996; Cloetingh et al., 2002; Watts and Burov, 2003; Moisio and Kaikkonen, 2006; Xia et al., 2006), dynamic and kinematic processes of the mountain ranges and sedimentary basins formation (Sassi and Faure, 1996; Meijer et al., 1997; Coblentz et al., 1998; Bada et al., 1998; Andeweg et al., 1999) and the available seismic data (Richardson and Coblentz, 1994; Hu et al., 1996; Negredo et al., 1999; Jiménez Munt et al., 2001).

This study has two principal aims. The first one is to establish the necessary conditions to reproduce the magnitudes of crustal stresses (uniaxial, lithostatic and tectonic states) in a cross-section with a flat topography by the finite element method. The second one consists of determining the stress magnitudes in the selected zone bearing in mind the present relief, the rheological changes associated to different lithologies and the magnitude of tectonic stresses. In order to achieve these objectives, two types of stress models, which differ in their geometry and rheological parameters, have been analysed. In the first case, a rectangular cross-section and an average rheology of the upper crust have been assumed while, in the other one, the topographical profile and the three main lithologies that crop out in the Variscan basement along a section parallel to the maximum horizontal stress have been taken into account.

2. Geological setting

The Spanish Central System is a thick-skin Cenozoic intraplate mountain range in the centre of the Iberian Peninsula (De Vicente et al., 2007) with a NE–SW structural trend in its eastern segment and an E–W structural trend in its western extension. One of the main characteristics of the range is that it is not nucleated on any ancient (Mesozoic) extensional zone. The Spanish Central System is located between two Cenozoic intracontinental sedimentary basins, the Duero Basin in the north and the Tagus Basin in the south (Fig. 1). The borders between the Spanish Central System and these basins are formed by upper crustal thrust faults with opposite dips that uplift the range in a pop-up structure (Vegas et al., 1990; Ribeiro et al., 1990; De Vicente et al., 1996; De Vicente, 2004; De Vicente et al., 2007) (Fig. 1). The Southern Border Thrust dips steeply north at depth and flattens out towards the surface (Racero Baena, 1988; Gómez-Ortiz et al., 2005). During the Eocene, movement along the fault probably occurred parallel to its strike as a left lateral strike-slip fault, whereas from the Oligocene–Lower Miocene the movement occurred parallel to its dip as a thrust fault (De Vicente et al., 2007). The origin of the Spanish Central System has been related to the transmission of tectonic stresses from the Pyrenean and Betic margins of Iberia towards the interior (Capote et al., 1990; De Vicente et al., 1996). However, new paleostress reconstructions suggest that the Variscan basement was uplifted by the Pyrenean collision with the mechanically coupled African–Iberian plates (De Vicente et al., 2007). These compressions are the result of the N–S to NNW–SSE convergence of the Euro-Asiatic and African plates since the Eocene (Dewey et al., 1989). Studies on stress inversion of fault-slip data and earthquake focal mechanisms indicate that the maximum horizontal stress in the range is now orientated NW–SE to NNW–SSE (De Vicente et al., 1996; Herraiz et al., 2000; De Vicente et al., 2007). There are Quaternary paleoseismic structures in the Tagus Basin (Giner, 1996) but instrumental seismicity is moderate to low and is restricted to a depth of less than 10 km (De Vicente et al., 1996; Herraiz et al., 2000; Tejero and Ruiz, 2002; De Vicente et al., 2007; De Vicente et al., 2008).

At the studied sector of the Southern Thrust of the Spanish Central System, the basement rheology consists of the El Berrocal granite that intrudes the San Vicente granodiorite (297 ± 1 Ma) as part of an important late Variscan extensional tectonic event (Fúster and Villaseca, 1987; Doblas, 1989; Campos et al., 1996; CSN, 2000) (Fig. 2). The granitic stock is located within the Sierra de San Vicente pop-up, where the basement overthrusts the Tietar Basin in a northerly direction and the Tagus Basin in a southerly direction (Fig. 1). This narrow pop-up structure presents a NE–SW direction and can be found along the entire Southern Thrust up to the Iberian Chain (Fig. 1). The El Berrocal massif has a strong structural control as a result of the final stages of both the Variscan orogeny and the Alpine ones which built up the mountain range (Capote et al., 1990; De Vicente et al., 1996a). It is intensely fractured with a predominance of strike-slip and normal faults (Fig. 2a and b) (Doblas, 1989; Campos et al., 1996; Pérez-López et al., 2005). Two principal paleostress fields, deduced from stress inversion of fault-slip data and fractal analysis of fault distribution, characterize the stress evolution of the massif (CSN, 2000; Pérez-López et al., 2005): a) a N–S extensional field probably related to a Late Permian–Early Triassic tectonic event (240 ± 10 Ma), which produced an important system of dikes and quartz veins and E–W normal faults, N60E right lateral strike-slip faults and N120E left lateral strike-slip faults and b) an Alpine field (Eocene to present?) with a strike-slip regime and maximum horizontal stress orientated N160E, which basically shapes the present morphology of the massif and develops N160E normal faults, N120–140E right lateral strike-slip faults, N10–30E left lateral strike-slip faults and N60–70E thrust faults (Fig. 2c). The Spanish Central System Southern Thrust is related to this latter stress field (De Vicente et al., 1996).

3. Elastic rheology and stress magnitudes

The rheological behaviour of the continuous lithosphere is such that small strains, until a yield strength is exceeded, can be considered as elastic. This simplification of the deformation mode is justified in the crustal cross-sections presented here since they will evaluate the stress magnitudes that are due to time-independent strains. In the case of plane strain ($\varepsilon_3 = 0$), the principal stresses (σ_1, σ_2, σ_3) and strains (ε_1, ε_2, ε_3) are related by the elastic parameters ν and E, the

Please cite this article as: Martín-Velázquez, S., et al., Intraplate stress state from finite element modelling: The southern border of the Spanish Central System, Tectonophysics (2009), doi:10.1016/j.tecto.2009.03.024

Table 1
Rheological parameters of the modelled materials (Turcotte and Schubert, 1982; Pérez del Villar et al., 1996; Gómez-Ortiz et al., 2005).

Stress models	Young's modulus (Pa)	Poisson's ratio	Density (kg/m^3)
Models A, B, C, D (flat crust)	60E9	0.25, ~0.5	2800
Case 1 (homogeneous Berrocal)	40E9	0.25, ~0.5	2600
Cases 2 and 3 (heterogeneous Berrocal)			
El Berrocal granite	50E9	0.25, ~0.5	2650
San Vicente granodiorite	40E9	0.25, ~0.5	2700
Tagus Basin sediments	30E9	0.25, ~0.5	2400

Poisson's ratio and the Young's modulus respectively (Turcotte and Schubert, 1982):

$$\begin{aligned}\varepsilon_1 &= [(1+\nu)/E][(1-\nu)\sigma_1 - \nu\sigma_2]\\ \varepsilon_2 &= [(1+\nu)/E][\nu\sigma_1 - (1-\nu)\sigma_2]\\ \sigma_3 &= \nu(\sigma_1+\sigma_2).\end{aligned} \quad (1)$$

The two most common reference states of stress assumed in the absence of tectonic loads are the uniaxial strain state and the lithostatic state (McGarr, 1988; Engelder, 1993). The vertical or lithostatic stress (σ_Y) at the earth's crust arises from the overburden load in both reference states, and is determined from the density (ρ) of rocks (McGarr and Gay, 1978; Turcotte and Schubert, 1982; Twiss and Moores, 1992; Engelder, 1993):

$$\sigma_Y = \rho g y \quad (2)$$

where g is the gravity acceleration and y the rock thickness.

The uniaxial strain reference state assumes a zero horizontal deformation. The horizontal stresses (σ_X, σ_Z) are thus a function of the overburden load and the Poisson's ratio:

$$\sigma_X = \sigma_Z = [\nu/(1-\nu)]\sigma_Y. \quad (3)$$

The lithostatic reference state assumes that rocks have no shear strength and that all stress components are equal:

$$\sigma_X = \sigma_Z = \sigma_Y = \rho g y. \quad (4)$$

Nevertheless, observations of *in situ* stress orientations and magnitudes demonstrate that these expressions do not fully explain crustal stresses (McGarr and Gay, 1978; Zoback et al., 1980; Brudy et al., 1997; Reynolds et al., 2006). The actual state of stress in the lithosphere differs from these two reference states, for example, as a result of tectonic stresses arising from interactions at the boundaries of lithospheric plates (Turcotte and Schubert, 1982; Engelder, 1993; Caputo, 2005). Other natural processes such as topographic loading, thermoelastic loading and erosion unloading create local stresses that also cause deviations. Tectonic stress is only added to the horizontal components of the reference state in regions under shortening deformation in order to generate a tectonic state, in which the stress magnitudes will depend on the choice of the initial state. For the uniaxial state assuming plane strain, the horizontal stresses are (Engelder, 1993):

$$\begin{aligned}\sigma_X &= \sigma_{HMAX} = [[\nu/(1-\nu)]\rho g y] + \sigma_T\\ \sigma_Z &= [[\nu/(1-\nu)]\rho g y] + \nu\sigma_T.\end{aligned} \quad (5)$$

And, for the lithostatic state:

$$\begin{aligned}\sigma_X &= \sigma_{HMAX} = \rho g y + \sigma_T^*\\ \sigma_Z &= \rho g y + \nu\sigma_T^*.\end{aligned} \quad (6)$$

In these equations $\sigma_T > \sigma_T^*$, (or $\sigma_T = \sigma_T^*$, if $\nu = 0.5$), and both are expressions of tectonic stresses for different reference states. σ_{HMAX} is the maximum horizontal stress.

Estimates of the tectonic force producing lithospheric deformation ranges from 1×10^{12} to 5×10^{12} N m^{-1} (Kusznir, 1991; Coblentz et al., 1998; Govers and Meijer, 2001). These force values are equivalent to a range of tectonic stress from 10 to 50 MPa distributed in a 100 km thick lithosphere. Finite element models in the western Eurasian plate show that the best fitting for the present stress state in the Iberian Peninsula is obtained when applying a force along the Eurasian–African plate boundary that increases from ~0.1×10^{12} N m^{-1} near the Gloria Fault to ~1.5×10^{12} N m^{-1} in Tunisia (Gölke and Coblentz, 1996; Andeweg, 2002). The increase in forces from west to east results from the rotational convergence between Africa and Eurasia (Argus et al., 1989; DeMets et al., 1990, 1994; Rosenbaum et al., 2002; Stich et al., 2006). The intraplate tectonic maximum horizontal stress of Europe, estimated by these numerical models, is characterized by a NW–SE compression and a magnitude of 10–20 MPa. On the other hand, total strength of the Spanish Central System lithosphere, integrating rheological profiles, is 2.5–3$\times10^{12}$ N m^{-1} under compressive differential stresses, and 1.5–2.5$\times10^{12}$ N m^{-1} under tension (Tejero and Ruiz, 2002). This intraplate strength must balance the imposed tectonic stress at plate boundaries (Zoback and Townend, 2001).

4. Stress modelling

4.1. Effect of the Poisson's ratio and the horizontal load

A set of stress models with flat relief and a homogeneous crustal rheology was run in order to estimate the rheological parameters and boundary conditions that would best reproduce the reference and tectonic states. The 2-D model comprises a 50 km long and 10 km deep crustal section with elastic mechanical behaviour (Table 1). The mesh has 500 eight-node plane strain quadrilateral elements, with an average size of 1×1 km, and 1621 nodes (Fig. 3). With regard to boundary conditions, the vertical displacement of the base nodes was restricted and, for the models to be in equilibrium, the horizontal movement of the node located halfway in the base must also be fixed. Gravity acceleration ($g = 9.8$ m/s^2) and a compressive horizontal pressure in both lateral boundaries were applied, assuming that the vertical principal stress results from the lithostatic load (McGarr and Gay, 1978) and bearing in mind that numerical models in Iberia suggest that shortening must be included both from the north and south to produce coherent deformation patterns (Cloetingh et al., 2002). Different runs were made modifying size, rheological parameters and boundary conditions of the model. Only the results obtained on changing horizontal load and Poisson's ratio are detailed below, since they are the most important issues related to the variations of the stress magnitudes.

First, differences between loading the model with a horizontal load whose magnitude is calculated, on the one hand by the uniaxial equation (3) (model A) and on the other by the lithostatic stress (4) (model B), have been analysed. Contour diagrams of the vertical and horizontal stresses, using a Poisson's ratio of 0.25, are shown in Fig. 4. In both cases, σ_Y contours are parallel to the surface and their magnitudes increase with depth. σ_Y magnitude follows the relation $\rho g y$ in model A. However, σ_Y contours curve to the lateral boundaries

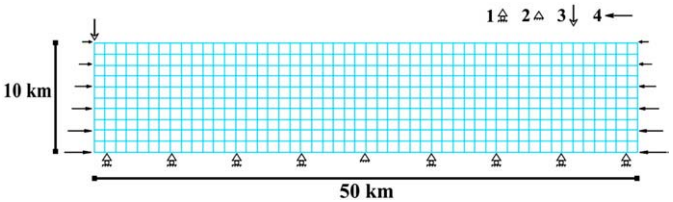

Fig. 3. Characteristics of the finite element mesh, boundary conditions and loads in the crustal cross-section with flat topography.

Please cite this article as: Martín-Velázquez, S., et al., Intraplate stress state from finite element modelling: The southern border of the Spanish Central System, Tectonophysics (2009), doi:10.1016/j.tecto.2009.03.024

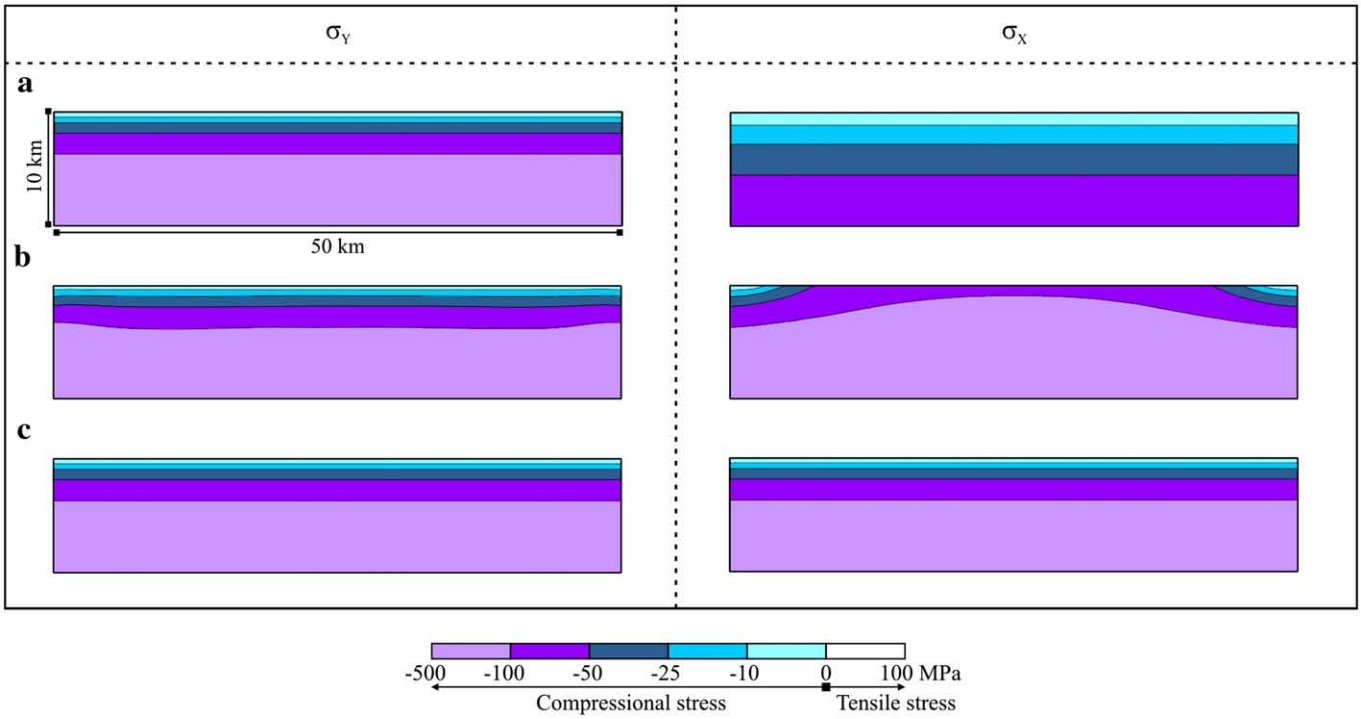

Fig. 4. Contour diagrams of the vertical (σ_Y) and horizontal (σ_X) stress magnitudes in the crustal cross-section with flat topography. a) Model A: uniaxial horizontal load and $\nu = 0.25$. b) Model B: lithostatic horizontal load and $\nu = 0.25$. c) Model C: lithostatic horizontal load and $\nu = \sim 0.5$.

in model B, indicating greater values in these areas. σ_X contours are also parallel to the topographic surface in model A and their magnitudes are equal to the uniaxial horizontal stress, whereas in model B they show a convex geometry and their magnitudes reach the lithostatic stress only towards the lateral boundaries.

Since a lithostatic state cannot be reproduced considering either of these two kinds of horizontal load and a Poisson's ratio of 0.25, a second analysis has been undertaken in which, the Poisson's ratio has been increased to ~0.5 and a load case is only considered, as the uniaxial load equals the lithostatic load (model C). With these new conditions, the contour diagram of $\sigma_Y = \sigma_X = \rho g y$ perfectly reproduces the lithostatic reference state (Fig. 4c).

Finally, the effect of tectonic stresses has been modelled by adding 20 MPa to the horizontal load of models A and C (model D). The magnitude of this extra-load is within the range collected in the previous section. σ_Y does not undergo any change, but the magnitude of σ_X increases 20 MPa in the entire model (Fig. 5). A $\sigma_H > \sigma_V$ (σ_H, horizontal stress; σ_V, vertical stress) tectonic regime is reached in the whole model from the lithostatic state as well as in the uppermost kilometre from the uniaxial state. For the latter case, a $\sigma_H < \sigma_V$ tensile regime prevails in the section.

4.2. Effect of topography and lithology

The influence of topographic load and lithological changes on stress magnitudes have been examined by means of several finite element models incorporating the El Berrocal massif. In one case, a uniform rheology for the upper crust is adopted, whereas in two others, the three main lithologies cropping out in the studied area are included. The underground pluton geometry and the basement depth in the Tagus Basin are based on a 2.5-D gravity model constrained with the geological and structural data exposed the surface, as documented in the following subsection.

4.2.1. Gravity modelling

In order to constrain deep geometries, a gravity study was carried out along a section that crosses the Southern Border Thrust of the Spanish Central System and the El Berrocal granite in a NW–SE direction, subparallel to the Alpine maximum horizontal stress (Fig. 2a). Bouguer anomalies were obtained from the published (ENRESA) gravity map of the Iberian Massif with 1 station/3 km (Muñoz Martín, 2004). The length of the cross-section was extended up to 200 km, to avoid boundary effects in the central part of the section. Published densities in Turcotte and Schubert (1982), Pérez del Villar et al. (1996) and Gómez-Ortiz et al. (2005) were used for surface lithological units (up to 4 km depth).

In the SE part of the section, the Bouguer anomalies show a strong gradient due to the density contrast between the igneous rocks of the

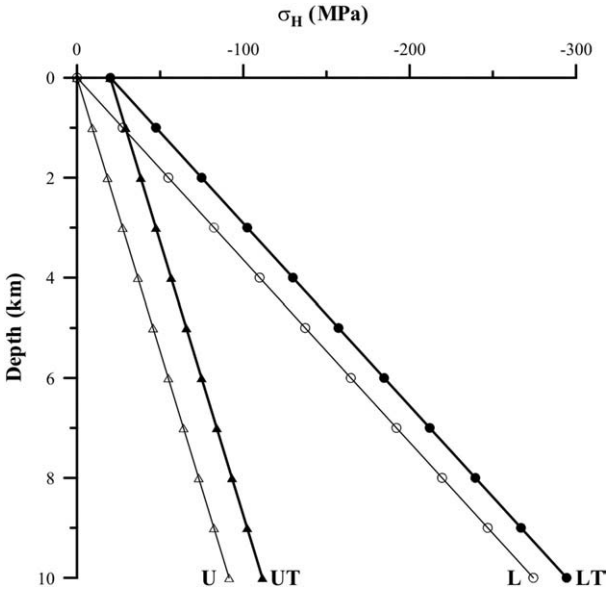

Fig. 5. Profiles of maximum horizontal stress *versus* depth in the crustal cross-section with flat topography for uniaxial load (U), uniaxial + tectonic (20 MPa) loads (UT), lithostatic load (L), and lithostatic + tectonic (20 MPa) loads (LT). The line L also represents the vertical lithostatic stress σ_V.

Please cite this article as: Martín-Velázquez, S., et al., Intraplate stress state from finite element modelling: The southern border of the Spanish Central System, Tectonophysics (2009), doi:10.1016/j.tecto.2009.03.024

Variscan basement of the Spanish Central System and the sedimentary rocks of the Tagus Basin (Fig. 6). Seismic reflexion profiles and well data indicate that metamorphic rocks prevail in the northern part of the Tagus Basin basement (Racero Baena, 1988; Querol, 1989). Although there are no available drill-core data to determine the lithology of the basin basement in the studied area, it is thought to be granodioritic in accordance with the igneous origin of the basement at this sector of the Spanish Central System and it has been modelled as a body with $\rho = 2700$ kg/m^3. A granitic wedge has been included in the basement under the fault plane in order to reduce the calculated gravity anomaly value, on the basis of geological mapping and structural. A good fit between the observed and calculated values of the Bouguer anomaly has been achieved with the geometries and densities of the modelled units. The contact between the mountain range and the sedimentary basin is a fault plane, the Southern Border Thrust, similar in geometry with its easternmost area (Racero Baena, 1988; Gómez-Ortiz et al., 2005). The inferred vertical throw of the Southern Border Fault is ~1000 m, and the basement deepens gradually to the south until sediment thickness reaches 1500 m in the innermost part of the basin. This sediment thickness is much lower than in the northeastern part of the basin, where 3500 m has been observed (Querol, 1989).

4.2.2. Stress modelling

The inset in the previous gravity profile shows the modelled section (Fig. 6). It has a length of 12.5 km and a maximum height of 1050 m, and it extends to a depth of 4 km. The elastic mesh is formed by 4162 plane strain quadrilateral elements of eight nodes (average size of 125 × 125 m^2), and 12,775 nodes (Fig. 7). Boundary conditions are similar to those in the previous analysis, i.e. the vertical displacement of the base and the horizontal movement of the base node located on the Southern Border Thrust have been fixed. Regarding the model loads, gravity and a compressive horizontal load in the lateral edges with a magnitude equal to the uniaxial (3) and lithostatic (4) stresses have been applied. An additional constant load has also been added to the horizontal load to simulate the tectonic stresses.

The intraplate stresses obtained for the model with a uniform rheology (case 1) are shown in Fig. 8. Vertical stress contour diagrams are similar to those already obtained in models A and C. They parallel the topographic surface, which again indicates an increase proportional to the depth which depends on the topographic load (Eq. (2)). However, the horizontal stress magnitude is slightly different, as it increases to a lesser degree in the central part of the model than in the lateral sectors. Nevertheless, small areas with tensile horizontal stress develop at the surface. Through the estimate of the σ_X/σ_Y ratio, it can be checked that large areas of both models are under a $\sigma_H < \sigma_V$ regime. Principal stresses from the uniaxial loading are in the vertical/horizontal ($\sigma_V = \sigma_1$ and $\sigma_H = \sigma_3$ or σ_2). Nevertheless, they are only orientated in the vertical/horizontal in the granitic massif and in the lateral boundaries from the lithostatic loading, although σ_1 tends to the vertical and σ_3 to the horizontal.

In order to examine the effect of lithological changes on the stress magnitudes, a similar model was constructed, in which the different material parameters for each rock type (case 2; Table 1) were incorporated: El Berrocal granite, San Vicente granodiorite and Tagus Basin sediments. The main differences between this analysis and the preceding one (case 1) are detected in the uniaxial horizontal load modelling, especially in the magnitude of the horizontal stress (Fig. 9). There is an extensive zone of tensile σ_X across the highest summit of the profile. The results of lithostatic horizontal load are similar to those of the homogeneous model ones (case 1), though magnitude variations are detected near the lithological contacts. Once more, the stress regime is $\sigma_H < \sigma_V$ and principal stresses do not undergo significant changes regarding the uniform models in both loading cases.

A pressure of 20 MPa has been added to the horizontal load (case 3) with the aim of analysing the effect of tectonic stresses presumed to originate at the convergent boundary between the Eurasian and African plates. This magnitude is in accordance with studies dealing with the tectonic stress magnitude in the interior of Iberia (Gölke and Coblentz, 1996; Andeweg, 2002; Tejero and Ruiz, 2002). The discontinuities of stress contours across the contacts are sharpened, and the σ_X magnitude increases by approximately 20 MPa (Fig. 10). If a lithostatic load is applied at the lateral boundaries, greater magnitudes of σ_X develop near the surface in valley areas with lithological contacts but not in summit areas. However, the most significant result of this case is that the stress regime is $\sigma_H > \sigma_V$ both in the uppermost part of uniaxial loading model and in the whole lithostatic loading model. On the whole, principal stresses are in the vertical/horizontal, except for the shallowest part of the sections where they are orientated parallel/perpendicular to the surface. For the uniaxial case, $\sigma_H = \sigma_1$ and $\sigma_V = \sigma_2$ or σ_3 in the upper part where $\sigma_H > \sigma_V$, whereas they rotate and finally permute ($\sigma_H = \sigma_2$ and $\sigma_V = \sigma_1$) towards the lower part where $\sigma_H < \sigma_V$. For the lithostatic case, principal stresses are almost coincident with the vertical/horizontal axes ($\sigma_H = \sigma_1$ and $\sigma_V = \sigma_3$).

5. Discussion

5.1. Stress states in finite element models

The uniaxial state is achieved if a uniaxial horizontal load is applied in the lateral boundaries of the model (model A). The horizontal

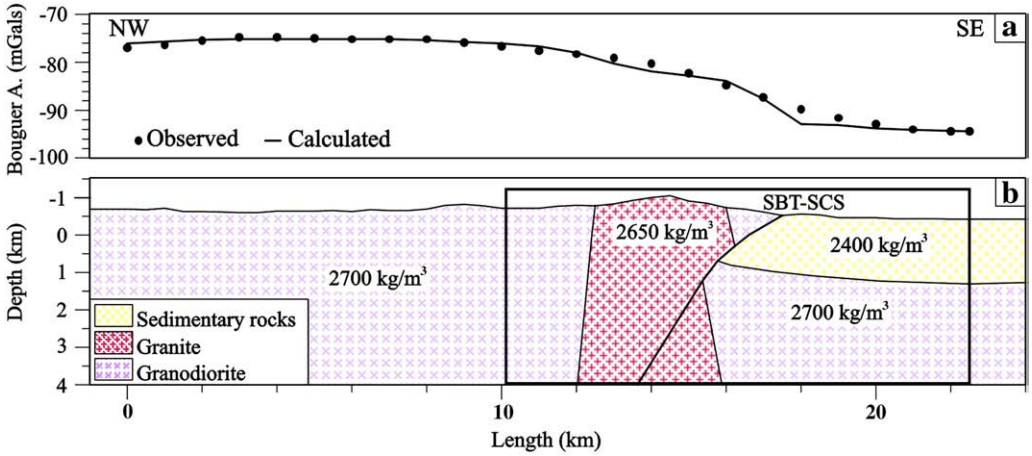

Fig. 6. 2.5-D gravity model of El Berrocal massif. a) Observed and calculated Bouguer anomaly. b) Deduced geological cross-section up to a depth of 4 km, where the density values used in the modelling are shown. The rectangle encloses the analysed section using finite element method.

Please cite this article as: Martín-Velázquez, S., et al., Intraplate stress state from finite element modelling: The southern border of the Spanish Central System, Tectonophysics (2009), doi:10.1016/j.tecto.2009.03.024

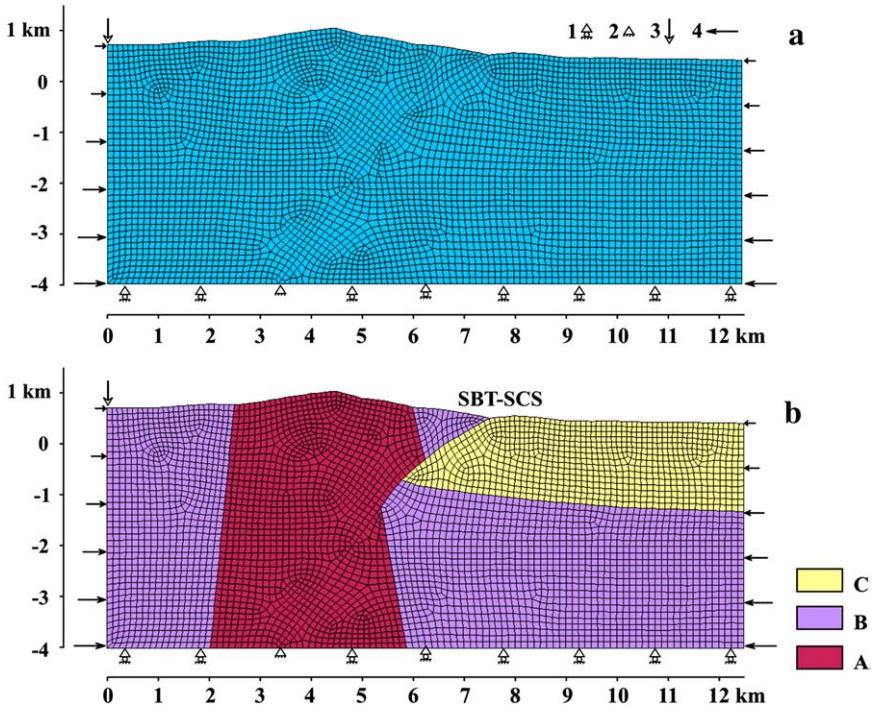

Fig. 7. Characteristics of the finite element mesh, boundary conditions and loads in the El Berrocal massif. a) Homogeneous rheology. b) Heterogeneous rheology. Lithologic legend: A. El Berrocal granite, B. San Vicente granodiorite, and C. sedimentary infill of the Tagus Basin. Symbol legend: 1. horizontal displacement, 2. fixed node, 3. gravity, and 4. horizontal load. SBF-SCS, Southern Border Fault of the Spanish Central System.

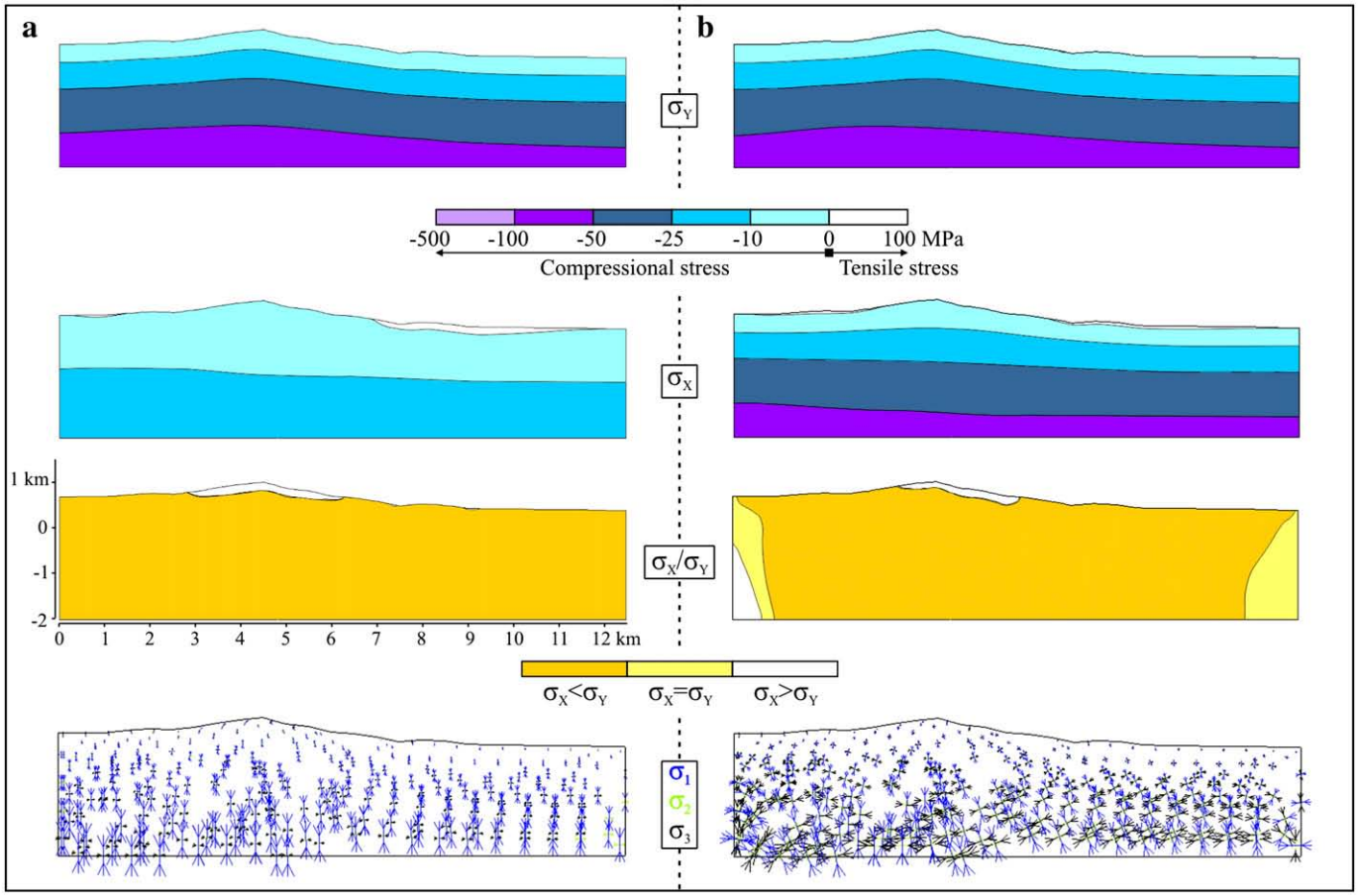

Fig. 8. Contour diagrams of σ_Y, σ_X, and σ_X/σ_Y, and tensors of σ_1, σ_2, σ_3 in the El Berrocal massif with a homogeneous rheology (case 1). a) Uniaxial horizontal load and $\nu = 0.25$. b) Lithostatic horizontal load and $\nu = \sim 0.5$.

Please cite this article as: Martín-Velázquez, S., et al., Intraplate stress state from finite element modelling: The southern border of the Spanish Central System, Tectonophysics (2009), doi:10.1016/j.tecto.2009.03.024

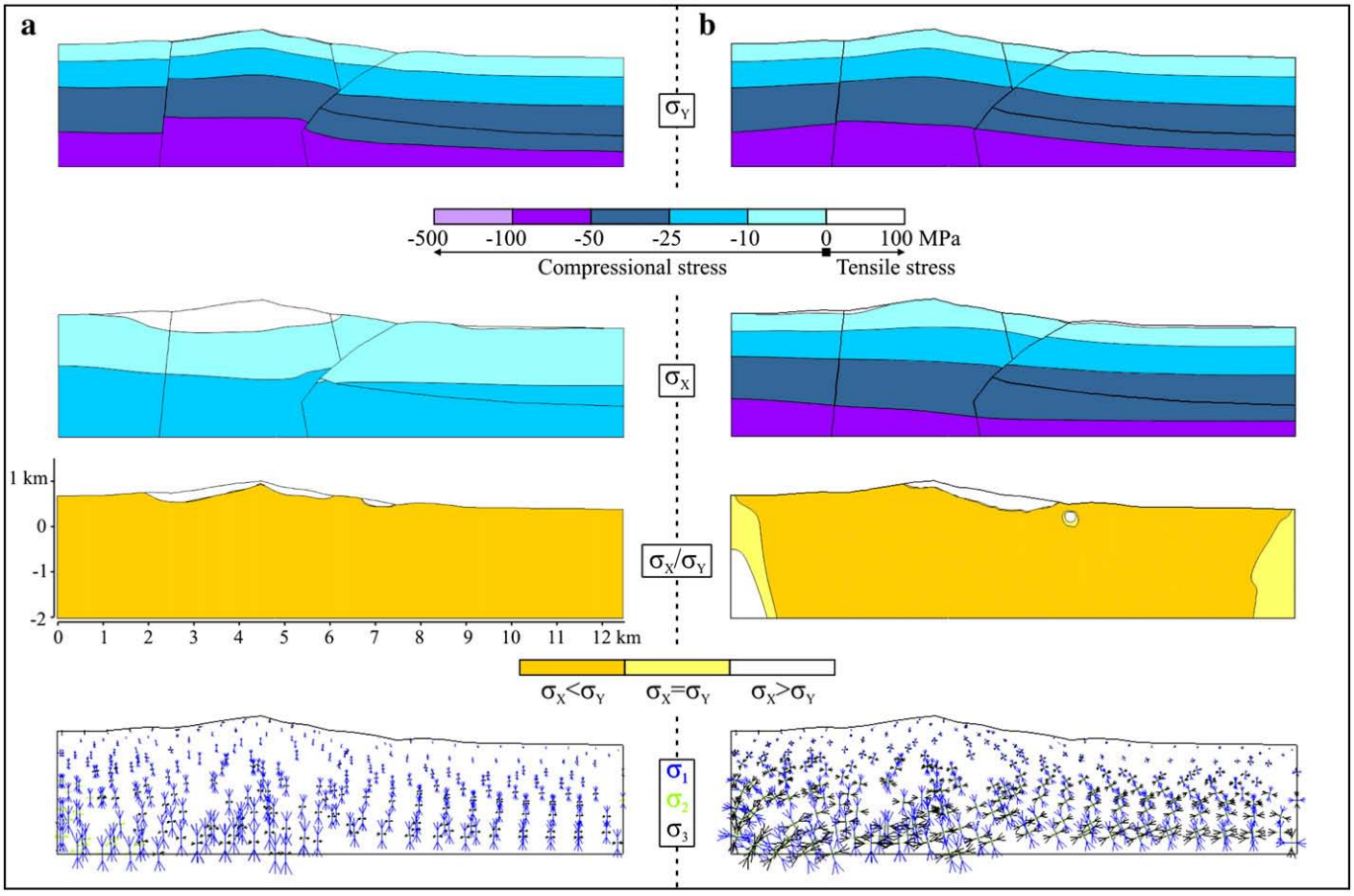

Fig. 9. Contour diagrams of σ_Y, σ_X, and σ_X/σ_Y, and tensors of σ_1, σ_2, σ_3 in the El Berrocal massif with a heterogeneous rheology (case 2). a) Uniaxial horizontal load and $\nu = 0.25$. b) Lithostatic horizontal load and $\nu = \sim 0.5$.

stresses balance the horizontal extension that is produced by the gravity load, and they are lower than the vertical stresses everywhere. The lithostatic state is only developed by increasing the Poisson's ratio to a value close to 0.5 (model C). In this case, the magnitudes of horizontal stresses in the upper 5 km of the central area of the model are greater than those of the vertical stress when $\nu = 0.25$ (model B). Although Poisson's ratio is very high compared with experimental data (Turcotte and Schubert, 1982; Twiss and Moores, 1992; Chevrot and van der Hilst, 2000; Punturo et al., 2005), this value must be used to simulate lithostatic state by trade packages of finite elements, as a consequence of the theory of elasticity in-plane strain (1). The simplification of the behaviour of the upper crust from 3-D to 2-D implies that: a) the lithostatic loads outside the cross-section are not included in the modelling, and b) the component of the stress tensor which is perpendicular to the cross-section is solved from the two in-plane stress components. Therefore, in the case of plane strain, the three normal stresses are equal when the value of Poisson's ratio is set to ~0.5. Wu (2004) also discusses this topic in numerical models with incompressible viscoelastic rheology. A tectonic state (model D) can be obtained simply by adding a constant horizontal load (20 MPa) to both reference states. The lithostatic model is defined by a widespread $\sigma_H > \sigma_V$ regime. However, a 20 MPa value is not sufficient to produce this tectonic regime in the whole uniaxial model and the stress state in its lower part is characterized by a $\sigma_H < \sigma_V$ regime.

5.2. Deviations from the stress reference states

The relief and the elastic properties of rocks create local components of stress whose effect is relatively small (Savage and Swolfs, 1986; Liu and Zoback, 1992; Twiss and Moores, 1992; Engelder, 1993; Caputo, 2005). Due to the topographic loading (case 1), a deviation from both reference states occurs. Horizontal stress magnitudes decrease below those deduced from Eqs. (3) and (4). Moreover, even vertical stress is slightly lower than the overburden stress (2). The σ_X/σ_Y diagrams show a widespread $\sigma_H < \sigma_V$ regime. When different lithological bodies are modelled (case 2), there are slight variations in the stress magnitudes, which are related to the new Young's modulus and density values, mainly associated with the Palaeozoic granite of the El Berrocal massif and the Tertiary sediments of the Tagus Basin. Nevertheless, the main deviation from the reference states arises from the tectonic load due to the African–Eurasian push force (case 3). The horizontal stress increase generates a change in the tectonic regime from $\sigma_H < \sigma_V$ to $\sigma_H > \sigma_V$, which involves the whole section from the lithostatic reference state and only the upper part from the uniaxial state.

5.3. Reference state: uniaxial versus lithostatic

Though various authors suggest that the most appropriate non-tectonic reference state of the lithosphere is that for which all three principal stresses are equal (Turcotte and Schubert, 1982; McGarr, 1988; Ranalli, 1995), several published works still discuss the approach of boundary condition of zero horizontal strain (Twiss and Moores, 1992; Engelder, 1993; Carminati et al., 2004). The most difficult component of the stress tensor to determine is the magnitude of maximum horizontal stress (Reynolds et al., 2006). However, direct measurements in deep wells, in regions which are geologically different, constrain the maximum horizontal stress to the following ranges: ~150–200 MPa at ~4 km depth in the Bohemian Massif (Brudy et al., 1997), ~140–160 MPa at ~5 km in the Baltic Shield (Lund and

Please cite this article as: Martín-Velázquez, S., et al., Intraplate stress state from finite element modelling: The southern border of the Spanish Central System, Tectonophysics (2009), doi:10.1016/j.tecto.2009.03.024

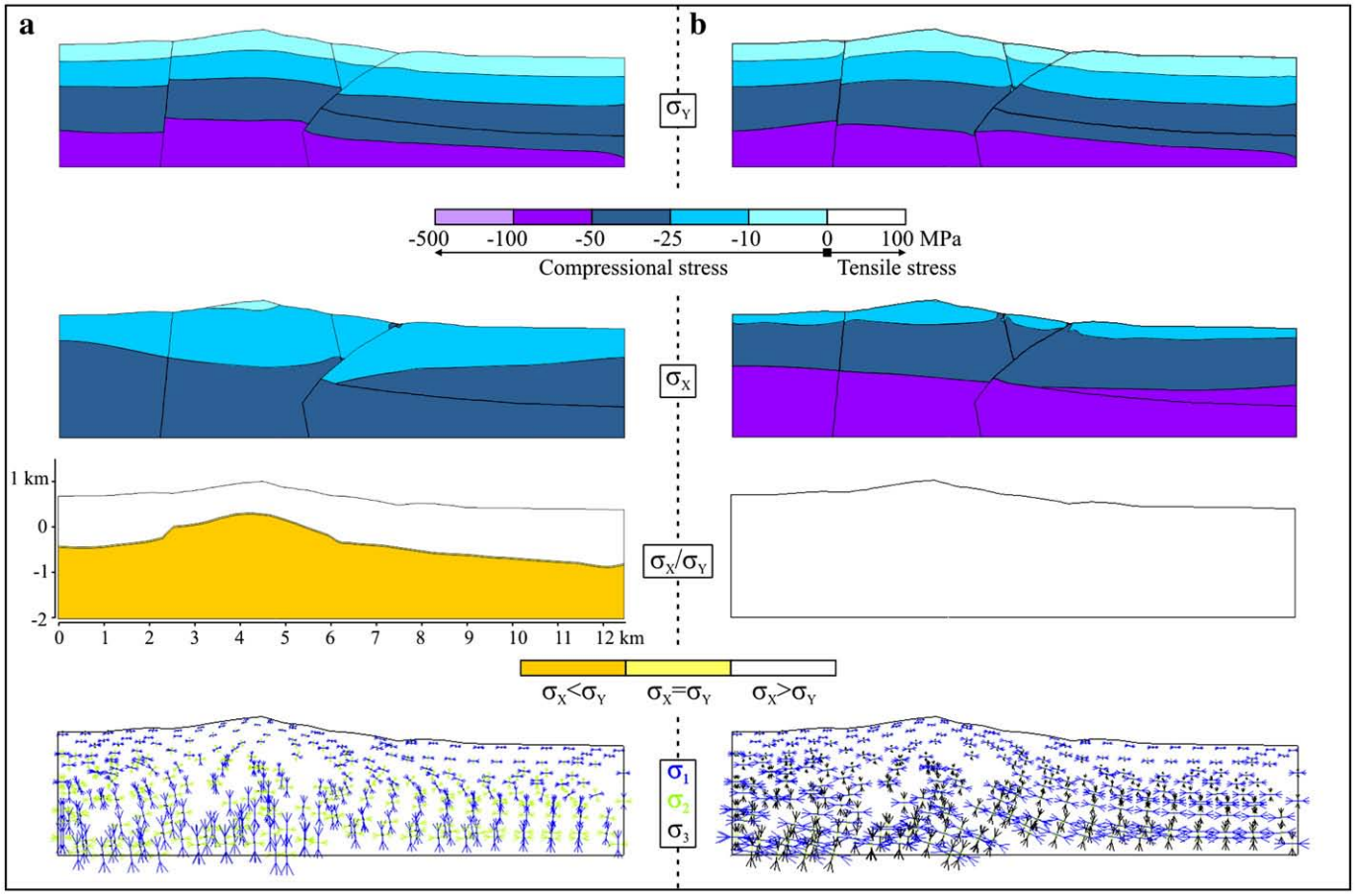

Fig. 10. Contour diagrams of σ_Y, σ_X, and σ_X/σ_Y, and tensors of σ_1, σ_2, σ_3 in the El Berrocal massif with a heterogeneous rheology (case 3). a) Uniaxial + tectonic horizontal load and $\nu = 0.25$. b) Lithostatic + tectonic horizontal load and $\nu = \sim 0.5$. The tectonic loading magnitude is 20 MPa.

Zoback, 1999), and ~105–115 MPa at ~3 km in the Cooper–Eromanga Basins (Reynolds et al., 2006). It should be noted that the stress measurements in wells are calculated using the pore pressure. Therefore, they describe the effective stress tensor, in which the magnitude of each of the normal components is reduced by an amount equal to the pore fluid pressure. Several studies indicate that the upper crust is specifically under hydrostatic pore pressure (see for example, Zoback and Townend, 2001). Although the numerical modelling presented here does not consider the decrease of the stress magnitude produced by this effect, the σ_H predicted by the models under a lithostatic state has a better correlation with the estimates in wells than the models under uniaxial strain state.

The Eocene–Present-day stress field in the studied area of the southern border of the Spanish Central System is characterized by a strike-slip regime with a maximum horizontal stress orientated NW–SE (CSN, 2000; Pérez-López et al., 2005). Although the stress models presented here are calculated under plane strain conditions (1) and taking into account that the principal stress tensors are in general orientated in the vertical/horizontal, the maximum stress tends to permute from the vertical to the horizontal axis when the tectonic load is added (cases 2–3; Figs. 9 and 10). With the aim of constraining the minimum tectonic load to produce a generalized $\sigma_H > \sigma_V$ regime in the cross-section of the southern Central System, its value was increased gradually. The transition from a $\sigma_H < \sigma_V$ to a $\sigma_H > \sigma_V$ regime is achieved over a range of 15–20 MPa from the lithostatic state, whereas an horizontal tectonic load greater than 65–75 MPa must be added from the uniaxial state. These magnitudes are in accordance with Eqs. (5) and (6). However, while the tectonic load from the lithostatic state is in the range of the intraplate tectonic stress, the estimated strength, and the tectonic force necessary to deform the Iberian lithosphere (Gölke and Coblentz, 1996; Andeweg, 2002; Tejero and Ruiz, 2002), the tectonic load from the uniaxial strain state is too large. Therefore, both the increase of σ_H with depth and the magnitude of tectonic loading are consistent with the approach of an initial lithostatic state and rule out the uniaxial state.

5.4. Stresses in the Iberian intraplate

A range of 30–35 MPa km^{-1} is obtained for σ_H in the southern border of the Spanish Central System from a tectonic load of 15 MPa added to the lithostatic initial state, and it decreases for lower loading values. The studies on magnitudes of σ_H in the shallowest crust by using direct measurement techniques in several regions of the Iberian Peninsula with different lithologies and stress regimes (Pyrenees, Ebro Basin, Valencia Trough, Iberian Massif, Iberian Range), provide an usual range from 10–30 MPa km^{-1} and an upper limit of ~60 MPa km^{-1} (González de Vallejo et al., 1988; Jurado and Müller, 1997; Schindler et al., 1998). Consequently, the stress gradients calculated from the numerical modelling are consistent with the direct estimations in Iberia.

The current active tectonic regime of Iberia changes from a thrust-fault regime in the SW corner of the peninsula to a normal-fault regime in the NE corner (Jiménez Munt and Negredo, 2003; De Vicente et al., 2008). These two zones are linked by a region under strike-slip to uniaxial extensional tensorial conditions, where the minimum principal stress is orientated NE–SW and the medium and maximum principal stresses permute from NW–SE to the vertical. The Spanish Central System is located in this complex area and the recent stress field in the considered zone is coherent with this geodynamical setting (CSN, 2000; Pérez-López et al., 2005). The tectonic stress that has been required to simulate a change from a $\sigma_H < \sigma_V$ to a $\sigma_H > \sigma_V$ regime in the upper part of the crust is

Please cite this article as: Martín-Velázquez, S., et al., Intraplate stress state from finite element modelling: The southern border of the Spanish Central System, Tectonophysics (2009), doi:10.1016/j.tecto.2009.03.024

around 15–20 MPa. This estimation is coincident with the magnitudes of the intraplate tectonic horizontal maximum stress (10–20 MPa) caused by the tectonic forces ($0.1–1.5\times10^{12}$ N m^{-1}) that have been proposed to be acting along the Eurasian–African plate boundary (Gölke and Coblentz, 1996; Andeweg, 2002). As the tectonic stress is also in the same range of the total strength of the lithosphere of the Spanish Central System (1.5–3×10^{12} N m^{-1}; Tejero and Ruiz, 2002), slight variations in its magnitude can favour the permutations between principal stresses and originate the strike-slip to normal regimes in the centre of the Iberia intraplate. Therefore, both the lithostatic stresses and the far effect of the plate collision are responsible for the intraplate stress field in the studied setting, whereas the lithological variations only generate local stress deviations.

6. Conclusions

Stress modelling using the finite element method has allowed us a) to constrain the boundary conditions that are required to simulate stress states in the surface crust and b) to analyse the variations in the predicted stress magnitudes of the southern border of the Spanish Central System, which are originated by the present-day topography, the elastic properties of rocks and the magnitude of the tectonic load.

The finite element representations of the geology need to have an adequate constraint of the geometry, rheology and boundary conditions in order to get coherent results. To simulate uniaxial and lithostatic reference stress states by means of finite element modelling, uniaxial and lithostatic loads have to be applied respectively in the lateral boundaries, and a Poisson's ratio of ~0.5 has to be set for the lithostatic state. The topographic loading and the lithological changes originate deviations from the initial states. However, the most important deviations occur when adding a constant horizontal load to model a tectonic stress state. From the two reference state, the lithostatic state is supported by the σ_H gradient calculated and the tectonic loading magnitude applied.

The stress modelling in the southern border of the Spanish Central System is consistent with the forces from the plate boundaries, the tectonic stress, the strength of the lithosphere, and the tectonic regime of Iberia (Gölke and Coblentz, 1996; Andeweg, 2002; Tejero and Ruiz, 2002; Jiménez Munt and Negredo, 2003; De Vicente et al., 2008). The tectonic state derived from the lithostatic state is the most suitable one for reproducing the intraplate stresses of Iberia. The magnitude of tectonic stresses is in the range of 15–20 MPa, which confirms earlier estimates of intraplate tectonic stresses for central Iberia. These values can produce permutations of the principal stresses and facilitate the coexistence of sectors under strike-slip and tension regimes in the Iberian intraplate, as deduced by active stress tensors. The σ_H gradient of 30–35 MPa km^{-1} is in the range of the direct measurements in the Iberian Peninsula (González de Vallejo et al., 1988; Jurado and Müller, 1997; Schindler et al., 1998).

Acknowledgements

We want to thank M. Sandiford, D. Coblentz, and an anonymous reviewer for their useful comments that helped to improve the manuscript. The study was supported by the Consolider Ingenio 2006 Topo IberiaCSD2006-00041 and the Spanish National Research Program CGL2006-13926-C02-01-02 Topo Iberia Foreland.

References

Andeweg, B., 2002. Cenozoic Tectonic Evolution of the Iberian Peninsula: Effects and Causes of Changing Stress Fields. PhD. Thesis, Vrije Universiteit, Amsterdam, 178 pp.

Andeweg, B., De Vicente, G., Cloetingh, S., Giner, J., Muñoz Martín, A., 1999. Local stress fields and intraplate deformation of Iberia: variations in spatial and temporal interplay of regional stress sources. Tectonophysics 305, 153–164.

Argus, D.F., Gordon, R.G., DeMets, C., Stein, S., 1989. Closure of the Africa–Eurasia–North America plate motion circuit and tectonics of the Gloria fault. J. Geophys. Res. 94, 5585–5602.

Bada, G., Cloetingh, S., Gerner, P., Horváth, F., 1998. Sources of recent tectonic stress in the Pannonian region: inferences from finite element modelling. Geophys. J. Int. 134, 87–101.

Brudy, M., Zoback, M.D., Fuchs, K., Rummel, F., Baumgärtner, J., 1997. Estimation of the complete stress tensor to 8 km depth in the KTB scientific drill holes: implications for crustal strength. J. Geophys. Res. 102, 18453–18475.

Campos, R., Martín Benavente, C., Pérez del Villar, L., Pardillo, J., Fernández-Díaz, M., Quejido, A., De la Cruz, B., Rivas, P., 1996. Aspectos geológicos: Litología y estructura a escala local y de emplazamiento. Geogaceta 20, 1618–1621.

Capote, R., De Vicente, V., González-Casado, J.M., 1990. Evolución de las deformaciones alpinas en el Sistema Central Español. Geogaceta 7, 20–22.

Caputo, R., 2005. Stress variability and brittle tectonic structures. Earth Sci. Rev. 70, 103–127.

Carminati, E., Wortel, M.J.R., Meijer, P.Th., Sabadini, R., 1998. The two-stage opening of the western-central Mediterranean basins: a forward modeling test to a new evolutionary model. Earth Planet. Sci. Lett. 160, 667–679.

Carminati, E., Doglioni, C., Barba, S., 2004. Reverse migration of seismicity on thrusts and normal faults. Earth Sci. Rev. 65, 195–222.

Chevrot, S., van der Hilst, R.D., 2000. The Poisson ratio of the Australian crust: geological and geophysical implications. Earth Planet. Sci. Lett. 183, 121–132.

Cloetingh, S., Burov, E., Beekman, F., Andeweg, B., Andriessen, P.A.M., Garcia-Castellanos, D., De Vicente, G., Vegas, R., 2002. Lithospheric folding in Iberia. Tectonics 21. doi:10.1029/2001TC901031.

CSN, 2000. Proyecto HIDROBAP. Hidrogeología de medios de baja permeabilidad. Colección Otros Documentos CSN, ODE-04.12. CSN, Madrid. 238 pp.

Coblentz, D., Sandiford, M., 1994. Tectonic stress in the African plate: constraints on the ambient stress state. Geology 22, 831–834.

Coblentz, D., Richardson, R.M., Sandiford, M., 1994. On the gravitational potential of the Earth's lithosphere. Tectonics 13, 929–945.

Coblentz, D.D., Zhou, S., Hillis, R.R., Richardson, R.M., Sandiford, M., 1998. Topography, boundary forces, and the Indo-Australian intraplate stress field. J. Geophys. Res. 103, 919–931.

De Vicente, G., Giner, J.L., Muñoz Martín, A., González Casado, J.M., Lindo, R., 1996. Determination of present-day stress tensor and neotectonic interval in the Spanish Central System and Madrid Basin, Central Spain. Tectonophysics 266, 405–424.

De Vicente, G. (Ed.), 2004. Estructura alpina del Antepaís Ibérico. In: Vera, J.A. (Ed.), Geología de España. SGE-IGME, Madrid, pp. 587–634.

De Vicente, G., Vegas, R., Muñoz Martín, A., Silva, P.G., Andriessen, P., Cloetingh, S., González Casado, J.M., Van Wees, J.D., Álvarez, J., Carbó, A., Olaiz, A., 2007. Cenozoic thick-skinned deformation and topography evolution of the Spanish Central System. Glob. Planet. Change 58, 335–381.

De Vicente, G., Cloetingh, S., Muñoz-Martín, A., Olaiz, A., Stich, D., Vegas, R., Galindo-Zaldívar, J., Fernández-Lozano, J., 2008. Inversion of moment tensor focal mechanisms for active stresses around the microcontinent Iberia: tectonic implications. Tectonics 27. doi:10.1029/2006TC002093.

DeMets, C., Gordon, R.G., Argus, D.F., Stein, S., 1990. Current plate motions. Geophys. J. Int. 28, 2121–2124.

DeMets, C., Gordon, R.G., Argus, D.F., Stein, S., 1994. Effect of recent revisions to the geomagnetic reversal time scale on estimates of current plate motions. Geophys. Res. Lett. 21, 2191–2194.

Dewey, J.F., Helman, M.L., Turco, E., Hutton, D.H.W., Knot, S.D., 1989. Kinematics of the western Mediterranean. Spec. Publ.-Geol. Soc. 45, 265–283.

Doblas, M.M., 1989. Estudio de las deformaciones tardihercínicas de los granitoides de un sector del Sistema Central Español (zona central de Gredos y áreas adyacentes). PhD. Thesis, Complutense University of Madrid, 465 pp.

Engelder, T., 1993. Stress Regimes in the Lithosphere. Princeton University, New York. 451 pp.

Fúster, J.M., Villaseca, C., 1987. El complejo tardihercínico del Sistema Central Español. In: Bea, F., Carnicero, A., Gonzalo, J.C., López Plaza, M., Rodríguez Alonso, M.D. (Eds.), Geología de los granitoides y rocas asociados del macizo hespérico. Libro homenaje L.C. García de Figuerola. Rueda, Alcorcón, pp. 27–35.

Galindo-Zaldívar, J., González-Lodeiro, F., Jabaloy, A., 1993. Stress and palaeostress in the Betic-Rif cordilleras (Miocene to the present). Tectonophysics 227, 105–126.

Giner, J.L., 1996. Análisis neotectónico y sismotectónico en el sector centro-oriental de la cuenca del Tajo. PhD. Thesis, Complutense University of Madrid, 345 pp.

Gölke, M., Coblentz, D., 1996. Origins of the European regional stress field. Tectonophysics 266, 11–24.

Gölke, M., Cloetingh, S., Coblentz, D., 1996. Finite-element modelling of stress patterns along the Mid-Norwegian continental margin, 62° to 68°N. Tectonophysics 266, 33–53.

Gómez, P., Turrero, M.J., Garralón, A., Peña, J., Buil, B., de la Cruz, B., Sánchez, M., Sánchez, D.M., Quejido, A., Bajos, C., Sánchez, L., 2006. Hydrogeochemical characteristics of deep groundwaters of the Hesperian Massif (Spain). J. Iber. Geol. 32, 113–131.

Gómez-Ortiz, D., Tejero, R., Ruiz, J., Babín-Vich, R., Rivas-Ponce, A., 2005. Crustal density structure in the Spanish Central System derived from gravity data analysis (Central Spain). Tectonophysics 403, 131–149.

González de Vallejo, L.I., Serrano, A.A., Capote, R., De Vicente, G., 1988. The state of stress in Spain and its assessment by empirical methods. In: Romana, M. (Ed.), Rock Mechanics and Power Plants. Proceedings of the ISRM Symposium. Balkema, Rotterdam, pp. 165–172.

Govers, R., Meijer, P.T., 2001. On the dynamics of the Juan de Fuca plate. Earth Planet. Sci. Lett. 189, 115–131.

Herraiz, M., De Vicente, G., Lindo Naupari, R., Giner, J., Simón, J.L., González Casado, J.M., Vadillo, O., Rodríguez Pascua, M.A., Cicuéndez, J.I., Casas, A., Cabañas, L., Rincón, P., Cortes, A.L., Ramírez, M., Lucini, M., 2000. The recent (upper Miocene to Quaternary) and present tectonic stress distributions in the Iberian Peninsula. Tectonics 19, 762–786.

Please cite this article as: Martín-Velázquez, S., et al., Intraplate stress state from finite element modelling: The southern border of the Spanish Central System, Tectonophysics (2009), doi:10.1016/j.tecto.2009.03.024

Hu, J.-C., Angelier, J., Lee, J.-C., Chu, H.-T., Byrne, D., 1996. Kinematics of convergence, deformation and stress distribution in the Taiwan collision area: 2-D finite-element numerical modelling. Tectonophysics 255, 243–268.
Jiménez Munt, I., Negredo, A.M., 2003. Neotectonic modelling of the western part of the Africa–Eurasia plate boundary: from the Mid-Atlantic ridge to Algeria. Earth Planet. Sci. Lett. 205, 257–271.
Jiménez Munt, I., Bird, P., Fernández, M., 2001. Thin-shell modeling of the neotectonics in the Azores–Gibraltar region. Geophys. Res. Lett. 28, 1083–1086.
Jurado, M.J., Müller, B., 1997. Contemporary tectonic stress in northeastern Iberia. New results from borehole breakout analysis. Tectonophysics 282, 99–115.
Kusznir, N.J., 1991. The distribution of stress with depth in the lithosphere: thermo-rheological and geodynamic constraints. In: Whitmarsh, R.B. (Ed.), Tectonic Stress in the Lithosphere. Royal Society, London, pp. 95–107.
Liu, L., Zoback, M.D., 1992. The effect of topography on the state of stress in the crust: application to the site of the Cajon Pass Scientific Drilling Project. J. Geophys. Res. 97, 5095–5108.
Lund, B., Zoback, M.D., 1999. Orientation and magnitude of in situ stress to 6.5 km depth in the Baltic Shield. Int. J. Rock Mech. Min. Sci. 36, 169–190.
McGarr, A., 1988. On the state of lithospheric stress in the absence of applied tectonic forces. J. Geophys. Res. 93, 13609–13617.
McGarr, A., Gay, N.C., 1978. State of stress in the earth's crust. Annu. Rev. Earth Planet. Sci. 6, 405–436.
Meijer, P.Th., Govers, R., Wortel, M.J.R., 1997. Forces controlling the present-day state of stress in the Andes. Earth Planet. Sci. Lett. 148, 157–170.
Moisio, K., Kaikkonen, P., 2006. Three-dimensional numerical thermal and rheological modelling in the central Fennoscandian Shield. J. Geodyn. 42, 95–114.
Muñoz Martín, A. (coord.), 2004. La estructura de la corteza del Antepaís Ibérico. In: Vera, J.A. (Ed.), Geología de España. SGE-IGME, Madrid, pp. 592–597.
Negredo, A.M., Barba, S., Carminati, E., Sabadini, R., Giunchi, C., 1999. Contribution of numeric dynamic modelling to the understanding of the northern Apennines. Tectonophysics 315, 15–30.
Pérez-López, R., Paredes, C., Muñoz-Martín, A., 2005. Relationship between the fractal dimension anisotropy of the spatial faults distribution and the paleostress fields on a Variscan granitic massif (Central Spain): the F-parameter. J. Struct. Geol. 27, 663–677.
Pérez del Villar, L., De la Cruz, B., Pardillo, J., Cózar, J.S., Pelayo, M., Marín, C., Rivas, P., Crespo, M.T., Galán, M.P., Reyes, E., Caballero, E., Delgado, A., Núñez, R., 1996. Estudios mineralógicos y litogeoquímicos de El Berrocal. Geogaceta 20, 1622–1625.
Punturo, R., Kern, H., Cirrincione, R., Mazzoleni, P., Pezzino, A., 2005. P- and S-wave velocities and densities in silicate and calcite rocks from the Peloritani Mountains, Sicily (Italy): the effect of pressure, temperature and the direction of wave propagation. Tectonophysics 409, 55–72.
Querol, R., 1989. Geología del subsuelo de la Cuenca del Tajo. Technical University of Madrid. 48 pp.
Racero Baena, A., 1988. Consideraciones acerca de la evolución geológica del margen NO de la cuenca del Tajo durante el Terciario a partir de los datos de subsuelo. In: SGE (Ed.), Proceedings of the II Congreso Geológico de España: Nuevas tendencias en el análisis de cuencas. SGE, Granada, pp. 213–221.
Ranalli, G., 1995. Rheology of the Earth. Chapman & Hall, London. 413 pp.
Reynolds, S.D., Mildren, S.D., Hillis, R.R., Meyer, J.J., 2006. Constraining stress magnitudes using petroleum exploration data in the Cooper–Eromanga Basins, Australia. Tectonophysics 415, 123–140.
Ribeiro, A., Kullberg, M.C., Kullberg, J.C., Manuppella, G., Phipps, S., 1990. A review of Alpine tectonics in Portugal foreland detachment in basement and cover rocks. Tectonophysics 184, 357–366.
Ribeiro, A., Cabral, J., Baptista, R., Matias, L., 1996. Stress pattern in Portugal mainland and the adjacent Atlantic region, West Iberia. Tectonics 15, 641–659.
Richardson, R.M., Coblentz, D.D., 1994. Stress modeling in the Andes: constraints on the South American intraplate stress magnitudes. J. Geophys. Res. 99, 22015–22025.
Rosenbaum, G., Lister, G.S., Duboz, C., 2002. Relative motions of Africa, Iberia and Europe during Alpine orogeny. Tectonophysics 359, 117–129.
Sassi, W., Faure, J.L., 1996. Role of faults and layer interfaces on the spatial variation of stress regimes in basins: inferences from numerical modelling. Tectonophysics 266, 101–119.
Savage, W.Z., Swolfs, H.S., 1986. Tectonic and gravitational stress in long symmetric ridges and valleys. J. Geophys. Res. 91, 3677–3685.
Schindler, A., Jurado, M.J., Müller, B., 1998. Stress orientations and tectonic regime in the northwestern Valencia Trough from borehole data. Tectonophysics 300, 63–77.
Stich, D., Serpelloni, E., Mancilla, F.L., Morales, J., 2006. Kinematics of the Iberia–Maghreb plate contact from seismic moment tensors and GPS observations. Tectonophysics 426, 295–317.
Tejero, R., Ruiz, J., 2002. Thermal and mechanical structures of the central Iberian Peninsula lithosphere. Tectonophysics 350, 49–62.
Turcotte, D.L., Schubert, G., 1982. Geodynamics. Applications of Continuum Physics to Geological Problems. John Wiley & Sons, Inc., New York. 450 pp.
Twiss, R.J., Moores, E.M., 1992. Structural Geology. W.H. Freeman and Company, New York. 532 pp.
Vegas, R., Vázquez, J.T., Suriñach, E., Marcos, A., 1990. Model of distributed deformation, block rotations and crustal thickening for the formation of the Spanish Central System. Tectonophysics 184, 376–378.
Watts, A.B., Burov, E.B., 2003. Lithospheric strength and its relationship to the elastic and seismogenic layer thickness. Earth Planet. Sci. Lett. 213, 113–131.
Wu, P., 2004. Using commercial finite element packages for the study of earth deformations, sea levels and the state of stress. Geophys. J. Int. 158, 401–408.
Xia, B., Zhang, Y., Cui, X.J., Liu, B.M., Xie, J.H., Zhang, S.L., Lina, G., 2006. Understanding of the geological and geodynamic controls on the formation of the South China Sea: a numerical modelling approach. J. Geodyn. 42, 63–84.
Zhou, S., Sandiford, M., 1992. On the stability of isostatically compensated mountain belts. J. Geophys. Res. 97, 14207–14221.
Zienkiewicz, O.C., Taylor, R.L., 1994. The Finite Element Method, vol. 1. McGraw-Hill, London. 648 pp.
Zoback, M.D., Townend, J., 2001. Implications of hydrostatic pore pressures and high crustal strength for the deformation of intraplate lithosphere. Tectonophysics 336, 19–30.
Zoback, M.D., Tsukahara, H., Hickman, S., 1980. Stress measurements in depth in the vicinity of San Andreas Fault: implications for the magnitude of shear stress at depth. J. Geophys. Res. 85, 6157–6173.

Please cite this article as: Martín-Velázquez, S., et al., Intraplate stress state from finite element modelling: The southern border of the Spanish Central System, Tectonophysics (2009), doi:10.1016/j.tecto.2009.03.024